Proc. 10th Int. Workshop on Neutrino-Nucleus Interactions in Few-GeV Region (NuInt15)
JPS Conf. Proc. **12**, 010008 (2016)
https://doi.org/10.7566/JPSCP.12.010008

Atmospheric Neutrino Flux Calculation with NRLMSISE-00 Atmosphere Model and New Cosmic Ray Observations

Morihiro Honda

Institute for Cosmic Ray Research, University of Tokyo, Kashiwa, Chiba, 277-8582 Japan.

E-mail: mhonda@icrr.u-tokyo.ac.jp

(Received January 27 2016)

We report here two recent developements of our calculation of atmospheric neutrino flux. One is the extension of calculation to the polar and tropical regions with NRLMSISE-00 global atmospheric model [1], and the other is a study of recent cosmis ray observations in terms of atmospheric neutrino flux. We have renewed the atmosphere model to NRLMSISE-00 global atmospheric model from the US-standard '76 atmospheric model [2]. It is well know that the atmophere profile in the polar region is largely different from that in mid-latitude region, and has a large seasonal variations. However, the US-standard '76 atmospheric model, which had been used in the calculation of atmospheric neutrino flux for a long time, has no positional or seasonal variations. The NRLMSISE-00 atmosphere global model represents the positional and seasonal variations on the Earth well. It is suitable for the calculation of atmospheric neutrino flux in the polar and tropical regions.
Apart from the atmosphere model, there has been impotant progresses in the observation of cosmic rays below 1 TeV by AMS02 [4] and BESS-polar [5]. There have been reported some observations of cosmic rays above 1 TeV, after we constructed our cosmic ray spectra model based on the observations of AMS01 [6] and BESS [7] observations. It is requested to study the atmospheric neutrino flux with new cosmic ray spectra model suggested by newer observations. On the other hand our interaction model is calibrated with the accurately observed atmospheric muon flux. With the new cosmic spectra model, we need to carry out the calibration with the muon flux, and calculate the atmospheric neutrino flux. Therefore, the difference of the cosmic ray spectra model does not direcly result in the difference of calculated atmospheric neutrino flux.

KEYWORDS: cosmic ray, atmospheric neutrino, hadronic interaction

1. Introduction

The experimental study of atmospheric neutrino has started in polar and tropical regions. On the other hand, the prediction of atmospheric neutrino flux at these sites are still poor. One of the reason for this situation is that the US-standard '76 atmosphere model, which has no time variation and no position dependence around the Earth, was generally used for a long time to calculate the flux of atmospheric neutrino. It is well known that there are large difference of air density profile between the polar regions and mid-latitude regions, and there is a large time variation in the polar region. Therefore, we looked for an advanced atmosphere model which expresses proper position dependence and the time variations on the Earth, to calculate the atmospheric neutrino flux in the polar and tropical regions, and find the NRLMSISE-00 global atmospheric model [1, 8].

Apart from the atmosphere model, there have been reported new measurements of cosmic ray spectra by AMS02 and BESS-polar, and they show a very good agreement in the energy region below 100 GeV. Adding to these, there have been carried out several cosmic ray observation experiment, after we constructed our primary cosmic ray spectra model. Sometimes it is requested to study the

difference when we use the cosmic ray spectra model based on the newer cosmic ray observations. However, as presently available data show a large scatter among different experiments above 1 TeV, it may be too early to renew our primary cosmic ray spectra model. Therefore, we construct a temporal cosmic ray spectra model, and study the difference of the atmospheric neutrino flux with the temporal spectra model from that calculated with our present one. By this study, we may understand the change of the atmospheric neutrino flux when we renew the primary cosmic ray spectra model.

In this paper, the basic calculation scheme is the same as our previous works [9–11] except for the atmosphere model. For the interaction model, we use DPMJET-III [12] above 32 GeV and JAM below that with the 'muon calibration' [10,11]. The IGRF geomagnetic field model [3], we have used so far in our calculation, is considered to be accurate enough in the polar and tropical (equatorial) regions where our target sites exist. We follow the motion of all the cosmic rays, which penetrate the rigidity cutoff as the primary cosmic rays and their secondaries. Then we examine all the neutrinos produced during their propagation in the atmosphere, and register the neutrinos which hit the virtual detector assumed around the target neutrino observation site.

We study in detail the atmospheric neutrino flux at the India-based Neutrino Observatory (INO) site (lat, lon)=(9°59′, 77°16′) for the tropical (equatorial) region, and the South Pole (−90°00′, 0°00′), and Pyhäsalmi (63°40′, 6°41′) mine (Finland) for the North polar regions in this paper. Also we compare the atmospheric neutrino flux calculated with the NRLMSISE-00 atmospheric model and that calculated with the US-standard '76 atmospheric model at Super Kamiokande (SK) site (36°26′, 137°10′).

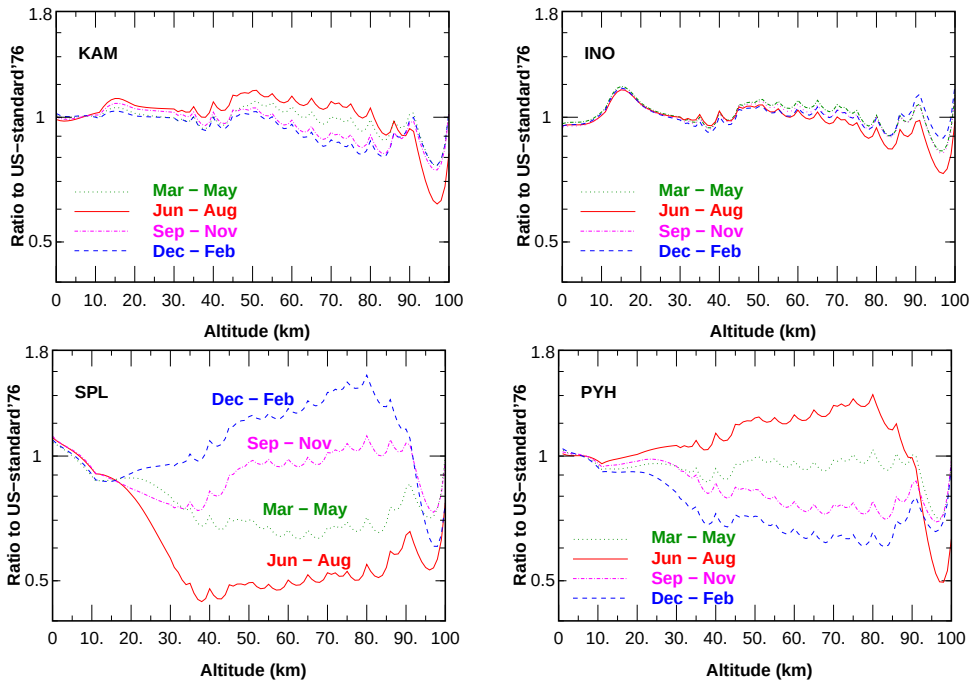

Fig. 1. The ratio of air density in the NRLMSISE-00 atmospheric model to that of US-standard '76 atmospheric model for the SK site (KAM), INO site (INO), South pole (SPL), and Pyhäsalmi mine (PYH), in the 4 seasons, March – May, June – August, September – November, and December – February.

2. NRLMSISE-00 atmosphere model

NRLMSISE-00 [1] is an empirical, global model of the Earth's atmosphere from ground to space. It models the temperatures and densities of the atmosphere's components.

However, the air density profile is the most important quantity in the calculation of atmospheric neutrino flux. We calculate the ratio of the air density in 4 seasons, March – May, June – August, September – November, and December – February at the SK site (KAM), INO site (INO), South pole (SPL), and Pyhäsalmi mine (PYH) by the NRLMSISE-00 atmospheric model to that by the US-standard '76 atmospheric model, and show it in Fig. 1 as a function of altitude.

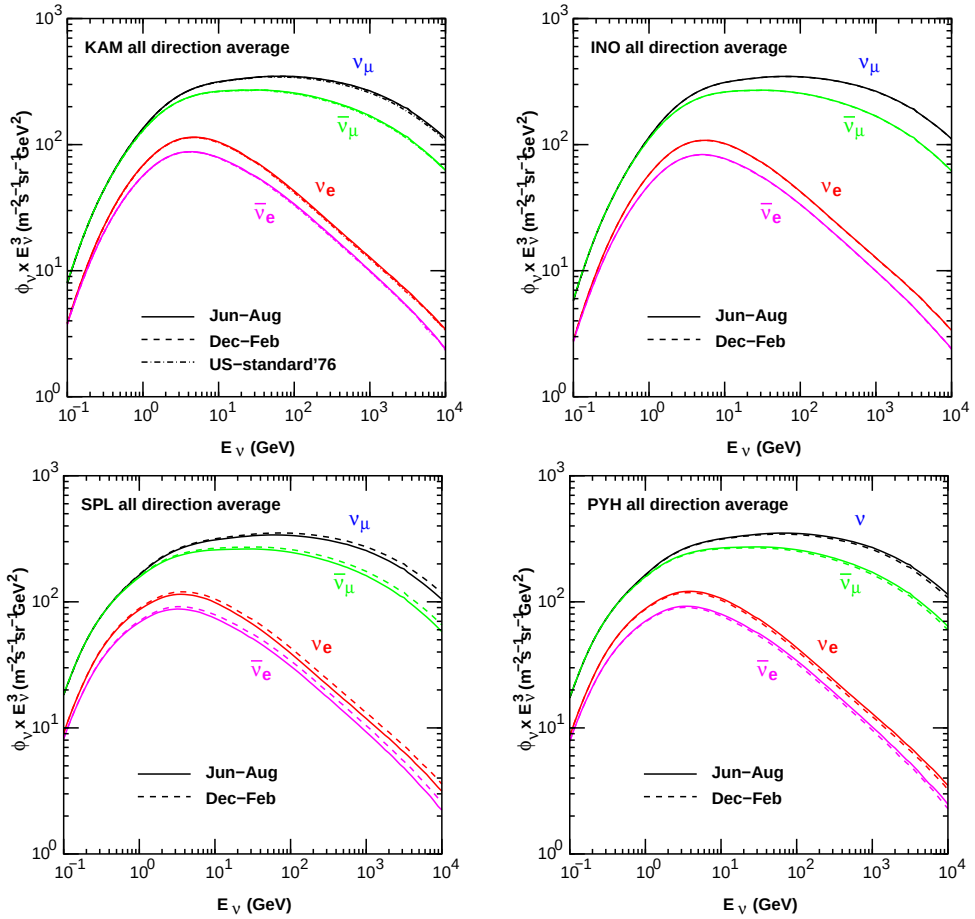

Fig. 2. All-direction averaged atmospheric neutrino flux for 4 sites. KAM stands for the SK site, INO for the INO site, SPL for the South Pole, and PYH for the Pyhäsalmi mine. The solid lines are the average in June – August, and dashed lines are in December – February. For the SK site, we also plot the result with the US-standard '76 atmospheric model in dash-dot below 1 TeV.

3. Atmospheric neutrino flux at each site

In Fig. 2, we show the time average of atmospheric neutrino fluxes over June – August and December – February at the SK site, INO site, South Pole, and Pyhäsalmi mine, averaging over all the directions. In the panel for SK site (KAM), we also depict the fluxes calculated with the US-

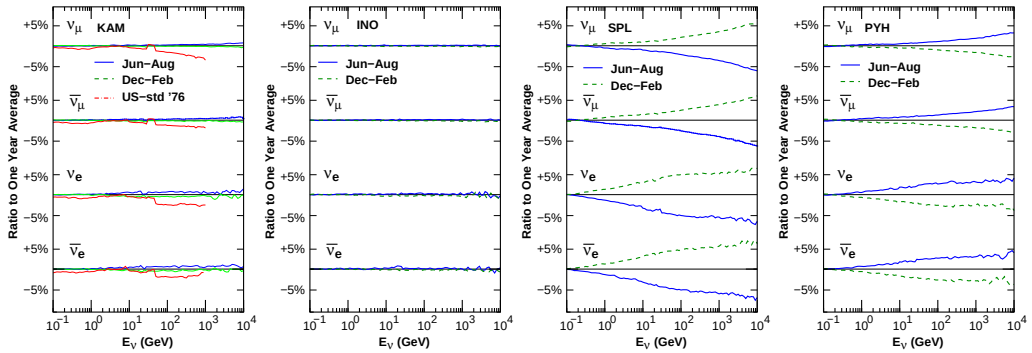

Fig. 3. Ratios of the all-direction averaged flux in June – August and in December – February to that of the yearly average. For the SK site, we also plot the ratio for the calculation with the US-standard '76 atmospheric model to the yearly average in dash-dot below 1 TeV.

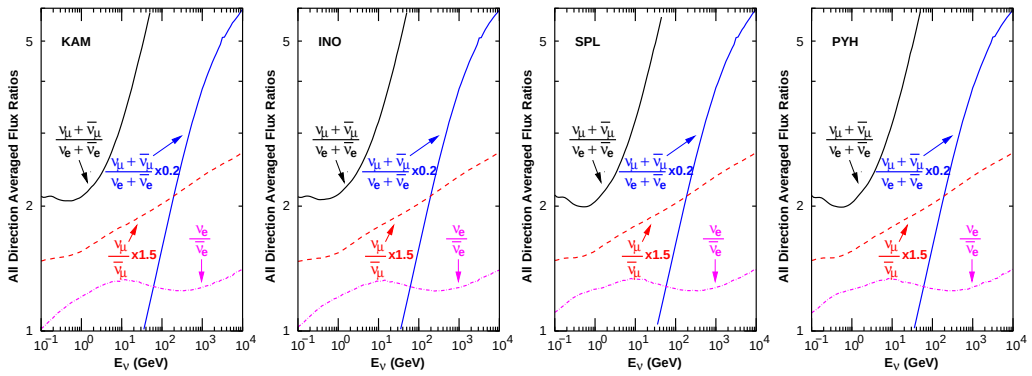

Fig. 4. Neutrino flavor-ratio calculated with the all-direction and one-year averaged atmospheric neutrino flux. KAM stands for the SK site, INO for the INO site, SPL for the South Pole, and PYH for the Pyhäsalmi mine.

standard '76 atmospheric model in the previous work [11] below 1 TeV only, as the statistics is poorer than the present work especially above 1 TeV.

The qualitative features are the same at all the sites. but we find a difference of flux among the sites by factor ~ 3 at the low energy end due to the large difference of the cutoff rigidity among these sites. The difference of flux between the two seasons (June – August and December – February) is seen in the panels for South Pole and for Pyhäsalmi mine, but is not clear in the panels for SK and INO sites.

3.1 Flavor-ratio of the atmospheric neutrino flux

In Fig. 4, we show the flavor-ratio defined by the flux ratio of different neutrino flavors, $(\nu_\mu + \bar{\nu}_\mu)/(\nu_e + \bar{\nu}_e)$, $\nu_\mu/\bar{\nu}_\mu$, and $(\nu_e/\bar{\nu}_e)$ at the SK site, INO site, South Pole, and Pyhäsalmi mine, averaging over all the directions. We find the flavor-ratio is very similar to each other among these sites, confirming the stability of the flavor-ratio. However, the flavor-ratio is an important quantities in the study of neutrino oscillations, we need to study the seasonal variations and position dependence's more precisely.

To see the seasonal variation of the flavor-ratio, we calculate the ratio of the flavor-ratio calculated with the all-direction and seasonally averaged fluxes to the that calculated with the all-direction and yearly average fluxes and plot them in Fig. 5 for each site. Also, to see the positional dependence

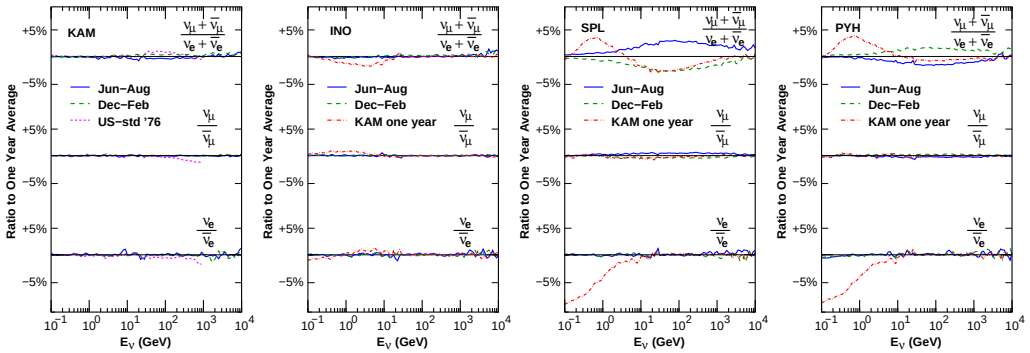

Fig. 5. Ratios of the flavor-ratio calculated with the all-direction and seasonally averaged flux to that calculated with all-direction and Yalu averaged flux. The solid lines are the flux ratio in June – August, and dashed lines are in December – February. KAM stands for the SK site, INO for the INO site, SPL for the South Pole, and PYH for the Pyhäsalmi mine. Taking the yearly averaged flavor-ratio at SK-site as the ''reference flavor-ratio", the ratio of ''reference flavor-ratio" to the yearly averaged flavor-ratio at each site are plotted with dash-dot other than the panel for the SK-site. In the panel for the SK-site, the ratio of the flavor-ratio with the US-standard '76 atmospheric model to the yearly averaged flavor-ratio at SK-site is plotted with dash-dot.

on the earth, we take the flavor-ratio calculated with the all-direction and yearly averaged fluxes at the SK site as the "reference flavor-ratio". Then we calculate the ratio of the "reference flavor-ratio" to those calculated with the all-direction and yearly averaged fluxes at each site, and plotted in the panel for each site of Fig. 5 except for SK-site. In the panel for the SK site, we show the ratio of the flavor-ratio calculated with the US-standard '76 atmospheric model to the ones calculated with all-direction and yearly averaged fluxes at the SK site (i.e. "reference flavor-ratio").

At the sites in the Polar region (South Pole and Pyhäsalmi mine), the flavor-ratio, $(\nu_\mu+\bar{\nu}_\mu)/(\nu_e+\bar{\nu}_e)$ shows a seasonal variation, high in summer and low in winter, with the maximum of the amplitude at $\sim$ 100 GeV. This is considered to be due to the seasonal variation of the altitude of cosmic ray interactions. Also the flavor-ratio shows some differences from the SK site at the energy below a few GeV. This is considered to be due to the lower air density at the neutrino production height of 10$\sim$20 km a.s.l in the Polar region. The smaller muon energy loss causes a smaller shifts of the energy spectra of the neutrinos produced in the muon decay .

Note, the air density at the South pole at the 10$\sim$20 km a.s.l. is much lower than at the Pyhäsalmi mine in Fig. 1, but the difference of the flavor-ratio, $(\nu_\mu + \bar{\nu}_\mu)/(\nu_e + \bar{\nu}_e)$ at the South Pole from the SK site is similar to that at the Pyhäsalmi mine. This is considered to be due to the higher observation site at the South Pole (2835m a.s.l.). The shorter distance from the ground to the production height of muons reduces the neutrino fluxes produced by muon decay at the South Pole.

In the $\nu_e/\bar{\nu}_e$ ratio, we also find a difference from the SK site at the South Pole and Pyhäsalmi mine, below a few GeV. This difference is considered to be due to the difference of cutoff rigidity. The $\nu_e/\bar{\nu}_e$ ratio reflects the π^+/π^- ratio of parent pions. As the majority of primary cosmic rays are protons, there is a π^+ excess generally. Especially when the cutoff rigidity is low enough, the pion production of primary cosmic rays overwhelms that of secondary cosmic rays, and π^+/π^- and $\nu_e/\bar{\nu}_e$ ratios are high even at low energies. However, when cutoff rigidity is high, the pion production by secondary cosmic rays can not be ignored, and the π^+ excess is diluted by the secondary neutron cosmic ray interactions.

In the comparison of neutrino flavor-ratio between the SK site (mid-latitude region) and the INO site (tropical region), we find a small difference in the $(\nu_\mu + \bar{\nu}_\mu)/(\nu_e + \bar{\nu}_e)$ ratio due to the difference of air density at 15 km a.s.l., and the difference of the muon energy loss. Other ratios are quite similar to each other. The differences of the flavor-ratio with the US-standard '76 atmosphere model are very

small to that in the present calculation.

4. Recent cosmic ray experiments and muon calibration

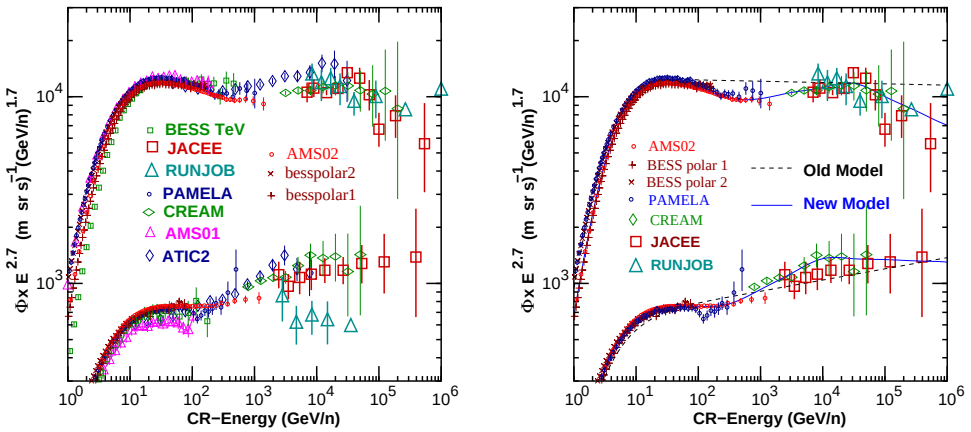

Fig. 6. Primary cosmic ray data and the spectra models. Left panel: Available data for cosmic ray protons and Helium's. AMS02 from Ref [4], besspolar1 and bessnpolar2 from Ref. [5], ATIC2 from Ref [13], PAMELA from Ref [14], JACEE from Ref [15], RUNJOB from Ref [16], CREAM from Ref [17], AMS01 from Ref [6], BESS TeV from Ref [18], Right panel: the temporal cosmic ray spectra model for cosmic ray protons and Helium's, and the data used in the model construction. The dashed line is the

Now we move to the second topic of this paper, the impact of the recent cosmic ray observation on the atmospheric neutrino flux calculation. In the left panel of Fig. 6, we summarized commonly referred cosmic ray data in the energy range from 1 TeV to 100 TeV. Recently the data from AMS02 and BESS-polar became available. They both, especially AMS02, have collected huge observation data and they agree each other within a few percent difference below 100 GeV. In the energy range from 100 GeV ti 1 TeV, the data of ATIC-2 [13], PAMELA [14], and AMS02 are available. Above a few TeV, there JACEE [15], RUNJOB [16], CREAM [17], and ATIC-2 data are available, but they show a large scatter among the experimental groups.

In the construction of the cosmic ray proton spectrum model, we used mainly AMS02 data below 1 TeV, since it achieved the highest statistics in the energy region and showed a remarkable agreement with the BESS-polar data below 100 GeV, except for the difference due to the solar modulation. We note that PAMERA also agrees with AMS02 within 5 % below 200 GeV, except for the difference below 10 GeV due to the solar modulation.

Above 1 TeV, ATIC-2, CREAM, and JACEE data are available. For proton cosmic rays, JACEE, RUNJOB, and CREAM data have an agreeable flux value at 10 TeV within each error bar. However, the ATIC-2 data for proton cosmic ray show a large difference from agreed flux vale of JACEE, RUNJOB, and CREAM. Also ATIC-2 data show a large difference form AMS02 even below 1 TeV. We used JACEE, RUNJOB, and CREAM data for spectrum model construction for the proton cosmic rays.

For Helium cosmic rays, we used mainly AMS02 data below 1 TeV, since it achieved the highest statistics in the energy region and showed a remarkable agreement with the BESS-polar data below 100 GeV, Above 1 TeV, JACEE, RUNJOB, CREAM, and ATIC-2 data are available. However, those data show a wider spread than those for cosmic ray protons. We used CREAM and JACEE data in this energy region, since they agree each other within the experimental error, and the extension of AMS02 data seems agree with those tow data.

Thus constructed primary spectra model for cosmic ray proton and Helium are plotted in the right panel of Fig. 6, with our present primary cosmic ray model. We note the maximum difference of two model reaches 20 % even below 10 TeV. The difference above 10 TeV could be large, but it would affect little in the calculated atmospheric neutrino flux below 100 GeV, which we consider the main target energy region of our calculation. There are heavier chemical compositions in the cosmic rays than the Helium. However, the contribution of heavier cosmic rays is relatively small to the atmospheric neutrino flux in the energy range we are working ($\lesssim$ 1 TeV). We use the spectra model for heavier cosmic rays with the proton and helium spectra model constructed here as the temporal cosmic ray spectra model.

In Fig. 7, We show the comparison in the all flavor sum, as the flavor ratio of neutrino is a stable quantity for the change of primary cosmic spectra model. we depict the ratio of the flux calculated with the temporal cosmic ray spectra model to that calculated with our present cosmic ray spectra model with solid lines for atmospheric muon (left) and neutrino (right), using the same interaction model for both calculations. We find there is $\sim$ 7 % decrease at $\sim$ 60 GeV for atmospheric muon flux, and at $\sim$ 30 GeV for atmospheric neutrino flux. This is due to the difference of the primary cosmic ray at $\sim$ 300 GeV for cosmic ray proton, and at $\sim$ 150 GeV for Helium cosmic rays. The difference at lower energy is due to the higher flux of Helium cosmic ray in the temporal model.

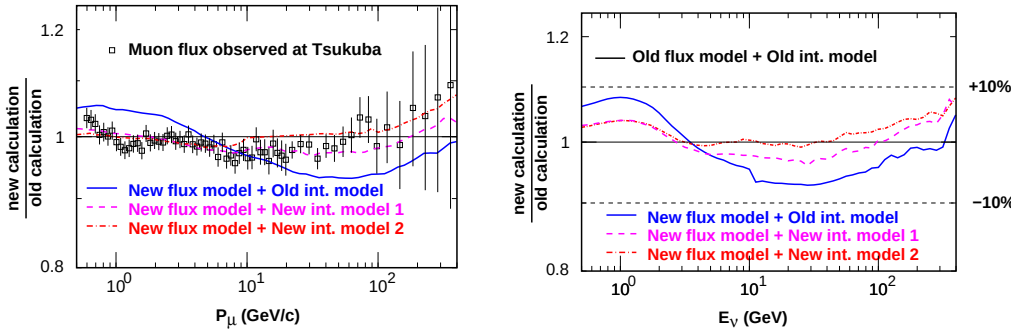

Fig. 7. Comparison of the atmospheric muon spectra (left panel) and atmospheric neutrino spectra (right panel) calculated using the temporal cosmic ray spectra model with those calculated using our cosmic spectra model. Solid lines show the calculation with our present interaction model, dashed and dash dot are calculations with the interaction models modified by the muon calibration with a little different conditions.

We note that the muon calibration is a key feature in our atmospheric neutrino calculation. We modify the interaction model so that it reproduce the accurately observed atmospheric muon flux, then calculate the atmospheric neutrino flux. When we replace the primary flux model, we should repeat the muon calibration with new primary flux model. Taking the muon spectra observed by BESS grope at Tsukuba [18] as the reference muon flux, we carry out the muon calibration, and modify the DPMJET-III and JAM interaction models, for the temporal primary spectra model. In the both panels of Fig. 7, we plot the calculated results with the muon calibrated interaction model (New int. model 1). Also we plot the results with similarly modified interaction model, but which gives the atmospheric neutrino flux closer to our present one (New int. model 2). The difference of the atmospheric neutrino fluxes with these interaction model from our present one is well smaller than 5 %. Note, even with our present interaction model, the calculated atmospheric neutrino flux with the temporal cosmic ray spectra model is within the allowed range by the uncertainty estimated in Ref [10].

5. Summary

We introduced the calculation of atmospheric neutrino flux with NRLMSISE-00 atmosphere model. We find the neutrino flux calculated with NRLMSISE-00 atmosphere model show some difference in Polar region from that in mid latitude region where Kamioka exist. Also there is a large seasonal variation in polar region even for flavor ratio of neutrino flux However, in mid latitude region, the difference in the calculations with NRLMSISE-00 atmosphere model and US-standard'76 are very small.

Apart from the atmosphere model, we studied the change of calculated atmospheric neutrino flux when we construct the primary cosmic ray spectra model with the recent cosmic ray observations by AMS02 and others. We find that the muon calibration of the interaction model absorb the change of primary cosmic ray spectra model, and result in a difference from our present calculated value even smaller than the estimated error of the calculation.

References

[1] J. M. Picone, J. Geophys. Res. **107**, SIA 15 (2002).
[2] See http://ccmc.gsfc.nasa.gov/modelweb/atmos/us_standard.html.
[3] See http://www.ngdc.noaa.gov/IAGA/vmod/igrf.html.
[4] M. Aguilar, et al. (AMS02) Phys. Rev. Lett., **114**, (2015) 171103, and Phys. Rev. Lett., **115**, (2015) 211101.
[5] K. Abe et al., arXiv:1506.01267 [astro-ph.HE]
[6] J. Alcaraz et al. (AMS-01), Phys. Lett. **B490**, (2000) 27.
[7] T. Sanuki et al. (BESS), Astrophys. J. **545**, (2000) 1135.
[8] M. Honda, et al., Phys. Rev. D **92**, (2015) 023004.
[9] M. Honda, et al., Phys. Rev. D **70**, (2004) 043008.
[10] M. Honda, et al., Phys. Rev. D **75**, (2007) 043006.
[11] M. Honda, et al., Phys. Rev. D **83**, (2011) 123001.
[12] S. Roesler, R. Engel, and J. Ranft(2000), hep-ph/0012252.
[13] A.D. Panov et al. (ATIC-2), B. Russ. Acad. Sci. Phys. **73**, (2009) 564.
[14] O. Adriani et al. (PAMELA), Science **332**, (2011) 69,
[15] K. Asakimori et al., (JACEE) Astrophys. J. **502**, (1998) 278.
[16] A.V. Apanasenko, et al., (RUNJOB) Astropart. Phys. **16**, (2001) 13.
[17] Y.S Yoon et al. (CREAM-I), Astrophys.J. **728**, (2011) 122.
[18] S. Haino et al. (BESS-TeV), Phys. Lett. B **594**, (2000) 35.